

# Binding configuration, electronic structure, and magnetic properties of metal phthalocyanines on a Au(111) surface studied with *ab initio* calculations

Y. Y. Zhang, S. X. Du,<sup>\*</sup> and H.-J. Gao<sup>†</sup>*Institute of Physics, Chinese Academy of Sciences, P.O. Box 603, Beijing 100190, China*

(Received 22 December 2010; revised manuscript received 12 May 2011; published 29 September 2011)

Binding configurations, interface electronic structures, and magnetic properties of 3*d* transition-metal phthalocyanine (*MPC*, where  $M = \text{Mn, Fe, Co, Ni, Cu}$  or  $\text{Zn}$ ) molecular systems on a Au(111) substrate are systematically investigated with first-principles density functional theory calculations using the Perdew-Wang (PW91) exchange-correlation functional. We also calculate the corresponding properties of freestanding molecules and make comparisons between these two cases. It is found that MnPc, FePc, and CoPc have a stronger binding configuration than that of NiPc, CuPc, and ZnPc. For the magnetic properties of the *MPC* molecules, it is not affected after molecular adsorption, except for CoPc. In addition, for the adsorption properties of FePc on Au(111), we find that the low adsorption energy and small energy differences between different configurations allow the FePc molecules to diffuse easily on a Au(111) substrate at certain temperatures.

DOI: [10.1103/PhysRevB.84.125446](https://doi.org/10.1103/PhysRevB.84.125446)

PACS number(s): 68.43.Bc

## I. INTRODUCTION

Molecule-metal systems have attracted much attention<sup>1-5</sup> not only because of fundamental interest<sup>1-3</sup> but also for potential applications in future electronic devices.<sup>4,5</sup> Among these systems, metal phthalocyanine (*MPC*) represents one of the most promising and versatile classes owing to its unique properties and thermal and chemical stability. In recent years, there has been a variety of work performed on metal-Pc systems. For example, Hipsps *et al.* presented the adsorption behavior of FePc, CoPc, NiPc, and CuPc on a Au(111) surface.<sup>6-8</sup> The Kondo effect and its manipulations in *MPC* on different surfaces [CoPc/Au(111),<sup>9</sup> FePc/Au(111),<sup>10</sup> and MnPc/Pb/Si(111)]<sup>11</sup> were reported. Petraki *et al.* studied the electronic structure of NiPc thin films on inorganic and organic substrates.<sup>12</sup> The energy-level alignment at organic semiconductor interfaces of 3*d* transition-metal phthalocyanines was systematically investigated by Grobosch *et al.*<sup>13</sup> The transport and vibration properties of *MPC*-metal substrate systems were also studied.<sup>14-17</sup>

In these studies, quantum mechanical calculations based on density functional theory (DFT) were employed to understand and predict the interface properties of *MPC*-metal systems. The electronic structures of free *MPC* molecules with 3*d* transition metals were studied with various exchange-correlation functionals.<sup>18-23</sup> It was found that a hybrid functional could successfully cancel the self-interaction errors (SIEs) and described the electronic structure very well for a single *MPC* molecule.<sup>18,19,23</sup> Carefully chosen nonempirical hybrid functionals such as the Heyd-Scuseria-Ernzerhof (HSE03) and Perdew-Becke-Ernzerhof (PBE0) functionals can also perform well in periodical systems.<sup>24,25</sup> But because they are expensive and time consuming to run, it is hard to use these functionals for calculations of large molecule-metal systems. For the moment, state-of-the-art DFT calculations of *MPC*-metal interfaces still mainly use semiempirical functionals. It was found that DFT calculations made with a generalized gradient approximation (GGA) functional sometimes agreed well with experimental results on the metal-substrate distance and the scanning tunneling microscopy (STM) images, especially for CoPc/Ag(111).<sup>26</sup> In this paper, we choose

the Perdew-Wang (PW91) functional and investigate the adsorption behavior of FePc on a Au(111) surface. The most stable adsorption configuration, the interaction between FePc and Au(111), and magnetic properties are systematically calculated and analyzed. After that we investigate other *MPC*/Au(111) systems ( $M = \text{Mn, Co, Ni, Cu,}$  or  $\text{Zn}$ ). We find that the adsorption energies of all the configurations are approximately several hundred meV, implying a weak interaction between the molecules and the substrate. Also, the adsorption has little effect on the magnetic properties of the molecules, except for CoPc. The substitution of the central metal ion changes the interface properties of *MPC*/Au(111). The results of FePc/Au(111) and CoPc/Au(111) calculated with the PW91 functional are compared with the published results,<sup>9,10,27-29</sup> which is helpful to better understand the configurations and electronic properties of the *MPC*/Au(111) system.

## II. SELECTION OF FUNCTIONAL AND CALCULATION METHOD

Various functionals were used in *MPC*-metal substrate calculations. Hu *et al.* calculated the electronic and magnetic properties of *MPC* on a Au(111) system (where  $M = \text{Mn, Fe, Co, Ni,}$  or  $\text{Cu}$ ) at the 6-31G\*\*/local spin density approximation (LSDA) level implemented in the DMol package.<sup>9,27</sup> However, because of the overbinding feature caused by the local density approximation (LDA) functional, the binding energies are  $\sim -3.5$  eV.<sup>27</sup> We also used the LDA functional to calculate the FePc/Au(111) system and obtained a binding energy of  $-3.6$  eV and a migration barrier of 0.19 eV, which yields strong binding and a hopping rate of  $\sim 10$  times/s at 77 K. As a comparison, a calculation using the PW91 functional gave weak binding and a migration barrier of 0.04 eV, corresponding to a hopping rate of  $\sim 10^{10}$  times/s. Experimentally, time-resolved tunneling spectroscopy found that the hopping rate was larger than  $10^6$  at 77 K.<sup>29</sup> Considering that the diffusivity was decreased by an electric field, we conclude that the PW91 functional could give a better description than that with the LDA for FePc/Au(111).

Compared with LDA, GGA is believed to give an under-binding picture on molecule-metal substrate systems. Therefore, many van der Waals (vdW)-involved methods have been used to improve the description of the dispersion part.<sup>30-32</sup> These methods have given excellent results in many systems, such as graphite systems and so on.<sup>33</sup> In the past three years, these methods have also been applied to the *MPC*-metal substrate.<sup>34,35</sup> In these studies, the vdW interaction induced a close molecule-substrate distance and then influenced the electronic structure at the interface. However, even though the dispersion corrected DFT method (DFT-D), in which vdW interaction is explicitly incorporated by using dispersion force field,<sup>30</sup> performs fairly well in  $\pi$ - $\pi$  packing systems,<sup>33</sup> it overbinds the molecules to the metal substrate<sup>32,36-38</sup> and sometimes overestimates the binding energy with an error that is larger than the underestimates of a PBE functional.<sup>37</sup> One example in which the DFT-D method might give a wrong conclusion is the CoPc/Cu(111) system. In this system, a modified DFT-D method gave a stronger binding energy than did LDA.<sup>35</sup> We tested the FePc/Au(111) system with the DFT-D method (Grimme 06 scheme<sup>30</sup> and parameters for gold were chosen to be the same as Ag). It was found that the DFT-D method predicts an adsorption structure similar to the LDA result, with an average FePc-substrate distance of 2.81 Å, while the binding energy is  $-11.4$  eV, which is stronger than that obtained from the LDA calculation. This result is similar to the CoPc/Cu(111) system.<sup>35</sup> The recently developed vdW-DF method<sup>31</sup> sometimes did not perform well in a molecule-metal interface either. According to published results, vdW-DF calculations predicted a binding distance between the aromatic molecules and Cu(111) substrate to be much larger than the experimental results.<sup>39,40</sup>

At the same time, the traditional GGA functional works well in some *MPC*-metal systems. Baran *et al.*'s calculated results of CoPc(SnPc)/Ag(111) using the PBE-GGA functional showed excellent agreement with experiments. Taking the SnPc/Ag(111) system as an example, the calculated 3.7-Å Pc-surface distance was relatively close to the experimental result (3.6 Å).<sup>26</sup> The Sn-surface distance also fit very well. In the PW91 functional, there is overbinding coming from the exchange part. Zhang *et al.* shows this will make the PW91 functional occasionally work fairly well in a vdW-dominated system.<sup>41</sup> Therefore, we used a PW91-GGA functional to make a systematic study of *MPC* ( $M = \text{Mn, Fe, Co, Ni, Cu}$  or  $\text{Zn}$ ) on a Au(111) surface, which may be helpful for to further understand the interaction between *MPC* molecules and the Au(111) substrate.

Quantum mechanical calculations were performed within density functional theory and the generalized gradient approximation using the VASP code.<sup>42,43</sup> Exchange-correlation effects were carefully checked and finally modeled using the Perdew-Wang functional (PW91).<sup>44</sup> The projector augmented-wave method was employed.<sup>45,46</sup> Periodic boundary conditions were applied. When calculating the properties of a free single molecule, a  $30 \text{ \AA} \times 30 \text{ \AA} \times 15 \text{ \AA}$  supercell was used. The *MPC* molecule was placed in the  $x$ - $y$  plane. When calculating the *MPC*/Au(111) systems, the supercell consisted of  $c(8 \times 7)$  repeated Au (111) slabs that were separated by 18 Å vacuum. We used four-layer gold atoms to model the substrate. The first two layers and the molecules are fully relaxed, which should

give a better description of the interaction between the central metal atom in *MPC* and the gold atom beneath it. This supercell consisted of 281 atoms. The electronic wave functions were expanded in plane waves with a kinetic energy cutoff of 400 eV.  $\Gamma$ -point  $k$  sampling was used. The structures were relaxed until the residual forces were smaller than  $0.02 \text{ eV/\AA}$ . Other parameters such as the smearing type were described when they were used. The calculated lattice constant for bulk Au was 4.174 Å. Comparing with the experimental result of 4.078 Å, there was a 2% discrepancy. The adsorption energy for *MPC* on Au(111) was defined as  $E_{\text{ads}} = E_{\text{MPC}/\text{Au}(111)} - E_{\text{MPC}} - E_{\text{Au}(111)}$ .

### III. FREESTANDING SINGLE MOLECULE

In order to investigate how the substrate influences the electronic structures and magnetic properties of *MPC* molecules, freestanding single *MPC* molecules were calculated first. Figure 1 shows the schematic structure of *MPC* ( $M = \text{Mn, Fe, Co, Ni, Cu,}$  or  $\text{Zn}$ ). Compared with  $\text{H}_2\text{Pc}$  molecule, the two central hydrogen atoms of  $\text{H}_2\text{Pc}$  are replaced by a  $3d$  transition-metal atom. The molecule can be treated as a cross, with each leg  $\sim 1.5 \text{ nm}$  long, depending on the type of central metal atom.

Spin-polarized calculations were carried out first for all six molecules. NiPc and ZnPc were found as  $S = 0$ , which means that these two molecules were not spin polarized. The spin quantum numbers of the other molecules were  $1/2, 1/2, 1,$  and  $3/2$  for CoPc, CuPc, FePc, and MnPc, respectively. It was the same with the calculations obtained using other methods<sup>18-20</sup> and can be explained by simple ligand field theory. As NiPc and ZnPc are not spin polarized, in the following we just perform the non-spin-polarized calculations. One interesting thing that should be mentioned here is the magnetic moment of the CuPc molecule. Previous calculations and experiments did not have

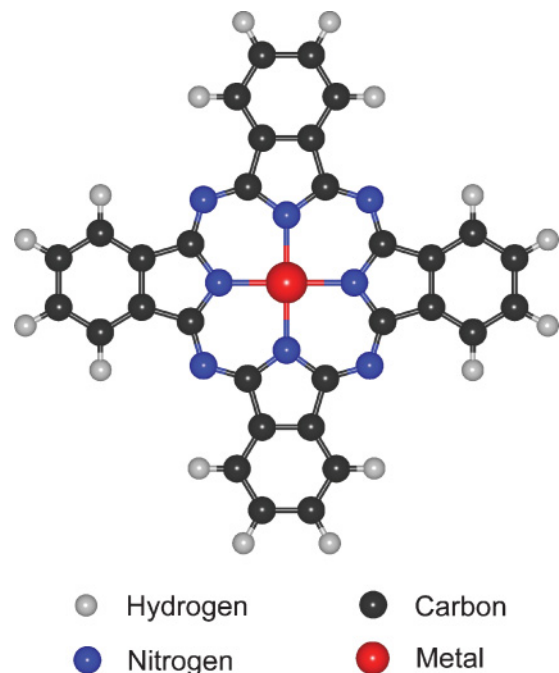


FIG. 1. (Color online) Schematic structure of  $3d$  transition metals *MPC* ( $M = \text{Mn, Fe, Co, Ni, Cu,}$  or  $\text{Zn}$ ).

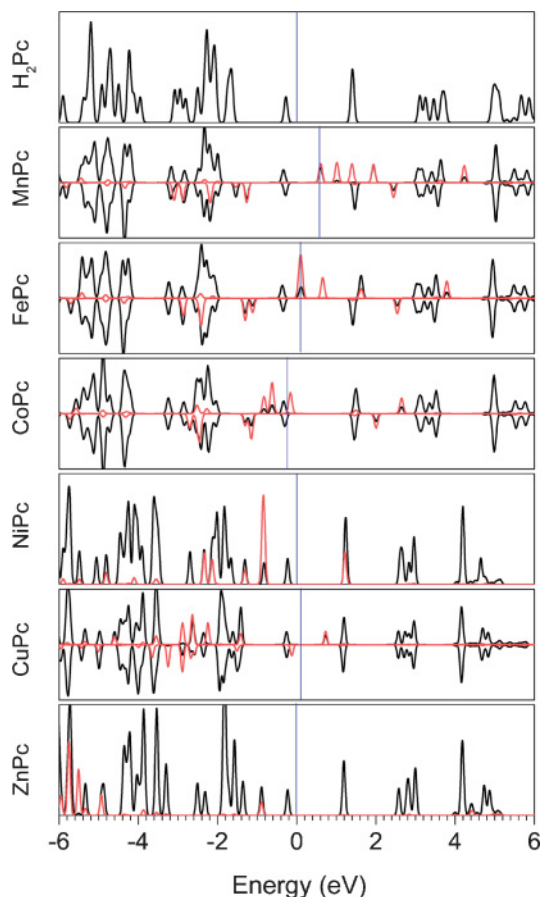


FIG. 2. (Color online) DOS of  $H_2Pc$  and PDOS of  $MPc$ , which are projected on the Pc framework (black line) and metal atoms (red/light gray line). The HOMO of  $H_2Pc$  and corresponding orbitals of  $MPc$  are aligned. The Fermi level is marked as a blue (gray) line in each panel.

consistent results about whether the  $CuPc$  molecule was spin polarized and what was the total magnetic moment for a single  $CuPc$  molecule. In our calculation, we support that  $CuPc$  is an  $S = 1/2$  system and the magnetic moment is  $1\mu_B$ , which is the same as that given in Refs. 18–20 and is different from that given in Ref. 27.

The density of states (DOS) of a free  $MPc$  molecule is shown in Fig. 2. The black lines are the projected DOS (PDOS) on the Pc frame of  $MPc$ . The red (light gray) lines are the PDOS on the central metal atom. Gaussian smearing was used in these calculations and a width of 0.05 eV was adopted. To show the effect of different central atoms on the DOS, we aligned the highest occupied molecular orbital of  $H_2Pc$  and the corresponding orbitals of the other  $MPc$  molecules. The positions of the Fermi level for each molecule were marked with blue (gray) lines. The results show that the original highest occupied molecular orbital (HOMO) and lowest unoccupied molecular orbital (LUMO) contributed from the Pc skeleton were nearly unchanged, even though their geometric structures and electronic properties were changed as the central metal atom changed. We also drew the shape of the wave functions of these two orbitals (not shown here), and they exhibited the same shape as the corresponding ones of the  $H_2Pc$  molecule. Compared to the LUMO of the  $H_2Pc$  molecule, the correspond-

ing orbitals of  $MnPc$  and  $FePc$  are strongly spin polarized. The existence of the Fe or Mn atom also induces extra states coming from the metal atom in the band gap of the Pc skeleton. These states decrease the band gap in the molecular crystal. For  $CoPc$  and  $CuPc$ , the orbital corresponding to the LUMO of  $H_2Pc$  is only slightly spin polarized. The new states coming from the metal atoms in the original gap are close to the original HOMO and LUMO, which means that the gap of  $CoPc$  and  $CuPc$  is only slightly decreased compared to that of  $MnPc$  and  $FePc$ . For  $NiPc$  and  $ZnPc$ , which are not spin polarized, the existence of the central metal atom does not greatly influence the original electronic structures of the Pc skeleton. Comparing with the experimental data,<sup>18,19,23</sup> the occupied states of free  $MPc$  molecules are squeezed, due to the choice of the PW91 functional. The Jahn-Teller effect may change the  $D_{4h}$  symmetry to  $D_{2h}$  and thus influence the electronic structure, especially for the charged case.<sup>47,48</sup> This will cause disagreement between scanning tunneling spectroscopy (STS) and the calculated local density of states (LDOS) results, but the main essential experimental features can be reproduced.<sup>49</sup>

#### IV. $FePc/Au(111)$ SYSTEM

$Au(111)$  is a well-investigated surface.<sup>50,51</sup> Its herringbone structure provides a good template for the adsorption of molecules and adatoms. At low coverage, molecules and atoms prefer to adsorb on the fcc packing region.<sup>52–54</sup> So an unreconstructed fcc packing slab model is a good approximation for studying the electronic properties of  $MPc$  on  $Au(111)$  at low coverage deposition. When one  $MPc$  molecule adsorbs on this fcc packing substrate, there are four typical adsorption sites: top, hcp hollow, fcc hollow, and bridge. While considering the angle between the lobe of a  $MPc$  molecule and the crystalline direction of the substrate, it becomes more complicated. Combining experimental results with the symmetry of the substrate and the molecule, we can get ten independent configurations, named as the top angle, top, bridge-I, bridge-II, bridge-III, bridge-IV, fcc, fcc angle, hcp, and hcp angle. This notation is also used below. Figure 3 is the top view of these ten configurations.

Because different stable configurations of  $FePc$  on  $Au(111)$  have been claimed in previous studies,<sup>10,27</sup> we first investigate the  $FePc/Au(111)$  system to point out the discrepancy. In this calculation, we used a PW91 exchange-correlation functional,

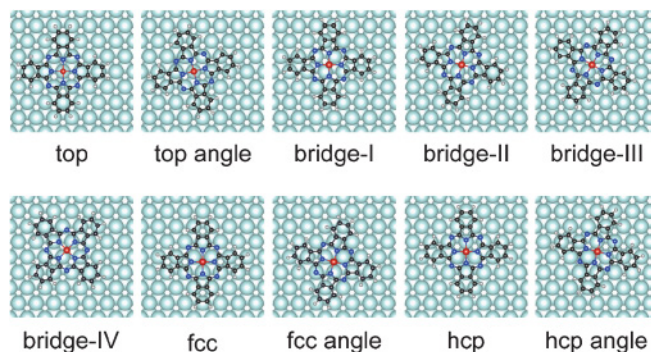


FIG. 3. (Color online) Typical adsorption configurations of  $MPc$  adsorbed on a  $Au(111)$  fcc terrace.

TABLE I. Properties of different configurations of FePc adsorbed on a Au(111) surface.

Index	$E_{\text{ads}}$ (eV)	$D_1$ (Å)	$D_2$ (Å)	$D_3$ (Å)
Top	-0.377	3.81	3.32	0.31
Top angle	-0.436	3.76	3.28	0.28
Bridge-I	-0.414	3.71	3.55	0.04
Bridge-II	-0.379	3.74	3.60	0.04
Bridge-III	-0.424	3.67	3.60	0.05
Bridge-IV	-0.407	3.76	3.70	0.03
fcc	-0.419	3.68	3.60	0.03
fcc angle	-0.397	3.88	3.81	0.03
hcp	-0.421	3.69	3.60	0.02
hcp angle	-0.403	3.87	3.78	0.02

a four-layer Au(111) substrate slab, Methfessel-Paxton order 1 smear type, with a width of 0.1 eV. The adsorption energies ( $E_{\text{ads}}$ ) and geometric parameters of different configurations are listed in Table I.  $D_1$  is the average vertical distance between the FePc molecule and the substrate.  $D_2$  is the vertical distance between the iron atom and the gold atom under it.  $D_3$  is the vertical distance between the highest gold atom (attracted by the iron atom) and the rest of the gold atoms in the first layer. We found that the top angle was the most stable configuration, which is in agreement with previous experimental observations and calculations given in Refs. 10, 28, and 29. The fcc, hcp, bridge-I, and bridge-III configurations were relatively metastable. So for other  $MPc/Au(111)$  systems, we just calculated and analyzed these five configurations. The adsorption energy differences between these states are small (several tens meV). It thus suggests that these configurations can coexist at certain temperatures, such as 300 K. The adsorption energy for the most stable adsorption configuration is  $-436$  meV. This adsorption energy is higher than that of a typical physical adsorption but is much lower than that of a chemical adsorption. The calculated migration barrier is 38 meV, which is large enough to make the molecule frozen at 4 K but is small enough to make it fast diffusing at 77 K; this conclusion has also been supported by the experiments in Refs. 28 and 29, which show that FePc diffuses easily on a Au(111) substrate at 77 K but gets fixed on the substrate at 4 K. The magnetic moment of a FePc molecule, before it is deposited on Au(111), is  $2\mu_B$ . While FePc is deposited on a Au(111) surface, our calculations still give a  $2\mu_B$  magnetic moment, which means the adsorption does not quench the spin of the FePc molecule.

These results are different from those given in Ref. 27, in which the most stable configuration is hcp hollow, the adsorption energy is much lower ( $-3.67$  eV), and the magnetic moment for FePc is half-quenched when adsorbed on Au(111). Comparing these with our calculation results, the differences could come from either the different exchange-correlation functionals or the different considerations for the substrate while relaxing the configurations. For different exchange-correlation functionals, we have checked our results using a LDA functional. The result shows that the most stable configuration is the top angle, which is the same as that obtained from the PW91 calculations. Different from PW91

calculation results, the magnetic moment changes to  $1\mu_B$  and the distance between the Fe and gold atoms is small. Therefore, the different exchange correlation functionals is the reason for the magnetic moment change. For the consideration of the substrate, the first two layers of the gold atoms were fully relaxed in our calculation while they were fixed in Ref. 27. After the first two layers of gold atoms were relaxed, some gold atoms were pulled out at a certain adsorption site. Taking the top-angle configuration as an example, the gold atom directly under Fe was lifted up as high as 0.3 Å in our PW91 calculation and 0.17 Å in our LDA calculation. This uplift of the Au atom will lower the energy of the system, and thus change the energy sequence between the different adsorption configurations. Therefore, it is clear that the fixation of the substrate contributes to the discrepancy of the most stable adsorption configuration between our calculation and the calculation in Ref. 27. A different choice of exchange-correlation functional contributes to the quench of the magnetic moment of the iron atom. As mentioned above, the LDA calculation gives a higher migration barrier as compared with the experiments. We can conclude that the choice of the functional and the relaxation of the first few layers under the adsorbed molecule are both very important for correctly understanding the electronic properties of the molecules on the substrate and the interaction between the molecules and the substrate.

The effect of different adsorption sites on the electronic structure was carefully analyzed. The projected DOS (PDOS) of a FePc molecule on each of several typical adsorption sites is shown in Figs. 4(a)–4(c). The PDOS of the Pc skeleton in each of these configurations is nearly the same and also is much the same as that in a free FePc molecule. This means

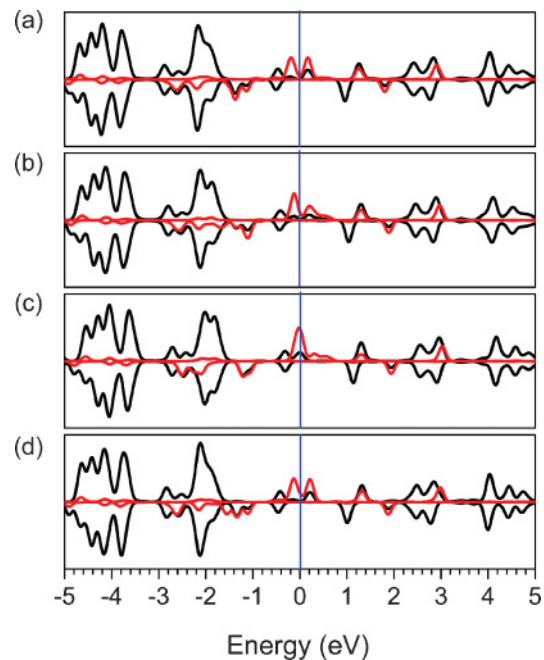


FIG. 4. (Color online) DOS of the FePc/Au(111) system with different adsorption configurations. The black lines are the PDOS on the Pc framework, and the red (gray) lines are the PDOS on the iron atom. (a) Top angle, (b) hcp, (c) bridge-III. (d) DOS of the configuration for one layer of FePc on Au(111).

that the interaction between the Pc and Au(111) is weak, and the adsorption has little influence on the electronic structure of the Pc skeleton. The PDOS of the Fe atom is different for different adsorption sites. It is also different from that of free FePc, especially near the Fermi level. This indicates that the interaction between the iron atom and the metal substrate is stronger than that between Pc and the substrate. This interaction is also site specific, which has been used to explain the site-specific Kondo effect.<sup>10</sup>

Charge transfer is an important aspect of molecular electronics. Here we also calculated the electron density difference in the FePc/Au(111) system. The electron density difference used here was defined as follows:

$$\Delta\rho = \rho_{MPc/Au(111)} - \rho_{MPc} - \rho_{Au(111)}.$$

Negative  $\Delta\rho$  means electrons loss, while positive  $\Delta\rho$  means electron accumulation.

Figure 5 shows the isosurfaces of the electron density differences of the most stable configuration in real space. Isosurfaces of  $\pm 0.002 \text{ \AA}^{-3}$  are selected, which is quite a small change in the FePc/Au(111) system. It is found that there is a small charge redistribution. For the Pc skeleton of a FePc molecule, the electrons in the  $p_z$  orbitals are transferred to the in-plane orbitals ( $p_x$  and  $p_y$ ). The conjugate properties are slightly weakened and the  $\sigma$  bonds in the molecular plane are enhanced. For the iron atom, the  $d_{xz}$  and  $d_{yz}$  orbitals are weakened and the  $d_{z^2}$  orbital is enhanced. A few electrons are transferred from the FePc molecule to the interface between the molecule and the substrate. This charge transfer forms a dipole pointing from the substrate to the molecule. The dipole moment in the top-angle configuration is  $\sim 1.32 \text{ eV \AA}$ .

The interaction between the adjacent molecules was also considered. A small supercell with a top-angle configu-

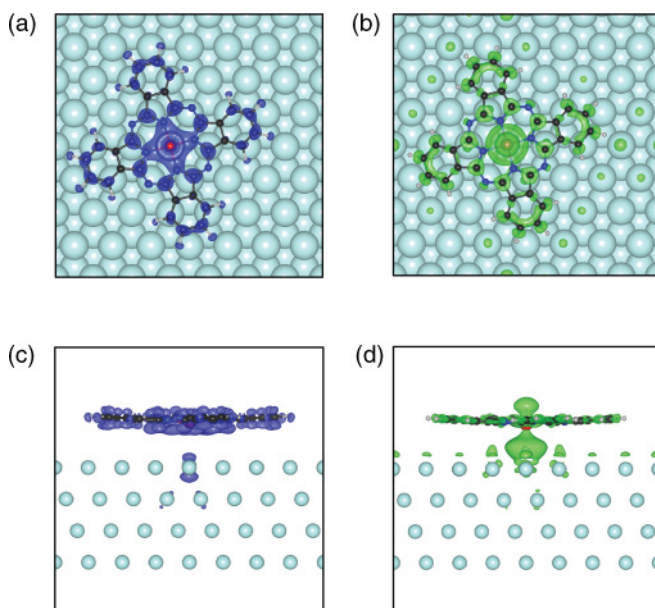


FIG. 5. (Color online) Isosurface of the electron density difference of the FePc/Au(111) system. (a) Top view and (c) side view of the negative isosurface of electron density difference.  $\Delta\rho = -0.002 \text{ \AA}^{-3}$ . (b) Top view and (d) side view of the positive isosurface of electron density difference.  $\Delta\rho = 0.002 \text{ \AA}^{-3}$ .

ration was used to simulate the monolayer structure of FePc/Au(111).<sup>53</sup> The parameters to optimize the structure and calculate the adsorption properties were the same as described above, but with a  $c(5 \times 6)$  supercell and a  $2 \times 2 \times 1$   $k$  sampling. The adsorption energy for this full-coverage system is  $-489 \text{ meV}$ , which is only  $53 \text{ meV}$  lower than that with a large supercell. The PDOS on the FePc molecule in the monolayer structure is shown in Fig. 4(d). Compared with that of single molecule adsorption [Fig. 4(a)], there are no obvious differences. All of this indicates that the interaction between the molecules is weak.

## V. OTHER MPc/Au(111) SYSTEMS

Since the PW91 calculation results of FePc/Au(111) agreed well with the experimental observations, such as the fast diffusion,<sup>28</sup> we performed similar calculations on other MPc/Au(111) systems ( $M = \text{Mn, Co, Ni, Cu, or Zn}$ ). The supercells used in these calculations were the same as those used in FePc/Au(111) calculations. For MnPc, CoPc, and CuPc, in which the freestanding molecules have a significant magnetic moment, we performed the spin-polarized calculations when we considered the adsorption on Au(111) surface. For NiPc and ZnPc, we tested whether they were spin polarized when adsorbed on the Au(111) surface. The calculations show that both the molecules and the substrate are not spin polarized. So we calculated these two systems without spin polarization.

First, the geometric structures were relaxed and the adsorption energies of the five selected adsorption configurations were calculated (see Table II). The average vertical distance between a MPc molecule and the Au(111) substrate ( $D_1$ ) for the most stable structure is  $3.77, 3.64, 3.84, 3.88,$  and  $3.68 \text{ \AA}$  for MnPc, CoPc, NiPc, CuPc, and ZnPc on Au(111), respectively. The gold atom beneath the metal atom is lifted up ( $D_3$ )  $0.35, 0.2, 0.04, 0.02,$  and  $0.02 \text{ \AA}$  and the metal-gold distance ( $D_2$ ) is  $3.00, 3.27, 3.78, 3.86,$  and  $3.56 \text{ \AA}$  for the same sequence, respectively. Here we find that the geometric distortion of MnPc, FePc, and CoPc is larger than that of NiPc, CuPc, and ZnPc, which means a stronger adsorption for MnPc, FePc, and CoPc molecules. These distances also suggest a relatively weak interaction between the molecules and the substrate.

For the spin-polarized systems (MnPc and CuPc) the magnetic moments of the adsorbed MPc molecules are not different than if the molecules were free. For CoPc, the magnetic moment changes from  $1\mu_B$  in a free molecule to  $0.58\mu_B$  after adsorption. As the adsorption energy of the CoPc/Au(111) system is smaller than that of MnPc/Au(111)

TABLE II. Adsorption energies of the MPc/Au(111) system in units of meV.  $E_{\text{ads}}^0$  is the adsorption energy of the most stable configuration. The others are relative energies compared with  $E_{\text{ads}}^0$ .

	$E_{\text{ads}}^0$	Top angle	Bridge-I	Bridge-III	fcc	hcp
MnPc/Au(111)	-533	0	44	15	39	26
FePc/Au(111)	-436	0	22	12	17	15
CoPc/Au(111)	-430	0	17	23	15	10
NiPc/Au(111)	-340	0	11	11	22	21
CuPc/Au(111)	-333	8	5	9	14	0
ZnPc/Au(111)	-327	16	0	16	5	1

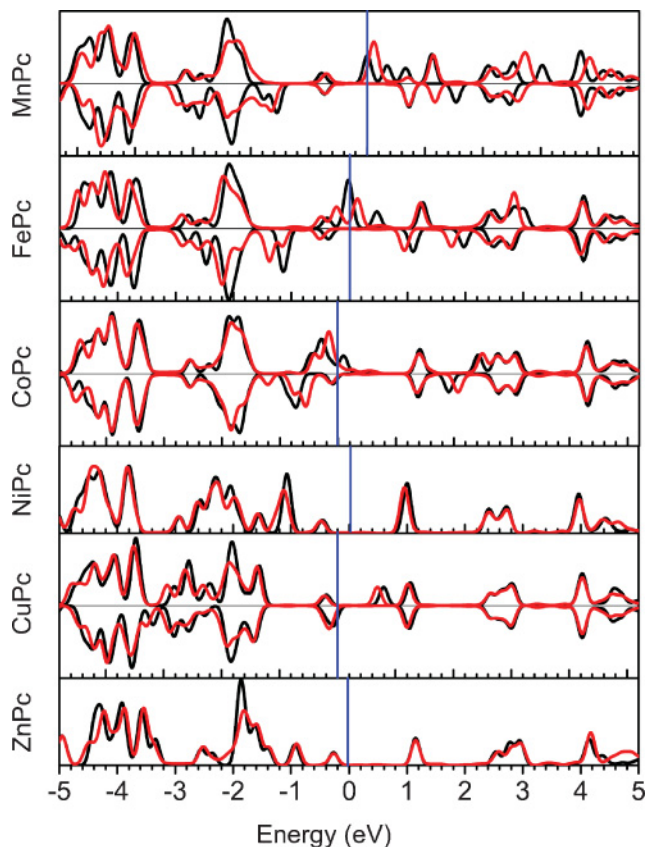


FIG. 6. (Color online) DOS of  $MPc$  and the  $MPc/Au(111)$  system. The black lines are the DOS of a free single  $MPc$  molecule. The red (light gray) lines are the DOS projected on the  $MPc$  molecule adsorbed on the  $Au(111)$  surface. The blue (gray) lines indicate the Fermi energy.

and  $FePc/Au(111)$ , indicating weaker binding between  $CoPc$  and the  $Au(111)$  substrate, this decreased magnetic moment is surprising. We then checked both smearing and  $k$  sampling. It was found that with a 0.02-eV smearing width and 13 irreducible  $k$  points, the magnetic moment increases to  $0.8\mu_B$ . These results indicate that the improper treatment of the fractional occupation near the Fermi level in the calculation may “cause” the decrease of the magnetic moment but not the adsorption. Whether the magnetic moment of  $CoPc$  is quenched by the adsorption or not should be further investigated by both experiments and theoretical calculations.

We also carefully analyzed the electronic properties of these systems and compared them with corresponding freestanding molecules. The DOS information before and after adsorption on the top-angle site is shown in Fig. 6. For  $MnPc$ ,  $FePc$ , and  $CoPc$ , the electronic states near the Fermi energy changed significantly, while for  $NiPc$ ,  $CuPc$ , and  $ZnPc$  they did not change that much. This means that the interaction between  $MPc$  ( $M = Mn, Fe, \text{ or } Co$ ) and  $Au(111)$  is stronger than that between  $MPc$  ( $M = Ni, Cu, \text{ or } Zn$ ) and the  $Au(111)$  substrate. This is consistent with the adsorption energies and the vertical distance between the central atom of  $MPc$  and the first layer of  $Au(111)$ . With regard to adsorption energy,  $MnPc/Au(111)$ ,  $FePc/Au(111)$ , and  $CoPc/Au(111)$  are relatively more stable than  $NiPc/Au(111)$ ,  $CuPc/Au(111)$ , and  $ZnPc/Au(111)$ .

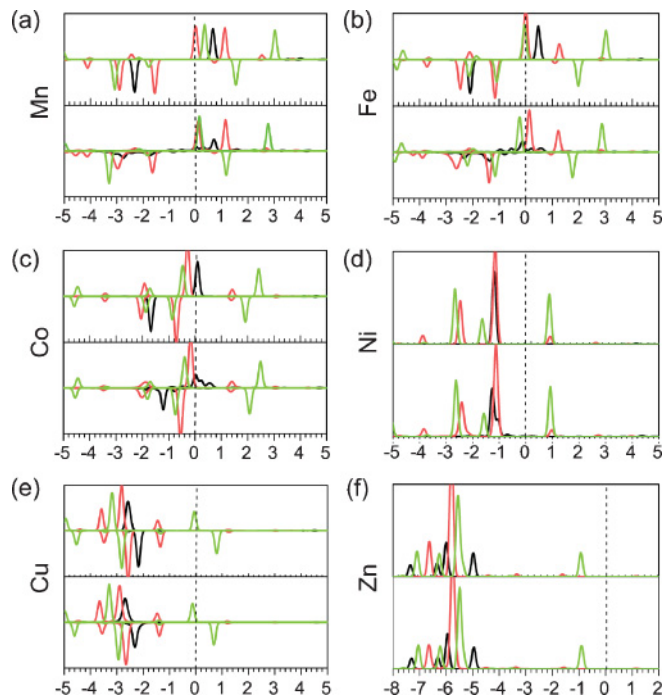


FIG. 7. (Color online) PDOS of the metal before and after adsorbed on a  $Au(111)$  surface. (a)  $MnPc$ , (b)  $FePc$ , (c)  $CoPc$ , (d)  $CuPc$ , (e)  $NiPc$ , (f)  $ZnPc$ . The upper panel in each figure is the PDOS of the metal atom in free  $MPc$ , and the lower panel is that after adsorption. The black lines are for  $d_{z^2}$  ( $m = 0$ ). The red (medium gray) lines are for  $d_{xz} + d_{yz}$  ( $|m| = 1$ ). The green (light gray) lines are for  $d_{xy} + d_{x^2-y^2}$  ( $|m| = 2$ ). The black dash lines indicate the Fermi energy.

Considering the vertical distances between the central metal atom and the gold atom underneath, we can conclude that the smaller is the distance, the more stable is the configuration.

Following from the discussion above, we find that the interaction between the central metal atom and the gold atom underneath it plays an important role in these systems, while the electronic structures of the  $Pc$  skeletons change only slightly. Figure 7 shows the PDOS of the central metal atoms before and after being adsorbed on top-angle sites. For all the  $MPc/Au(111)$  systems, the in-plane orbitals ( $d_{xy}$  and  $d_{x^2-y^2}$  orbitals,  $|m| = 2$ ) of the metal atoms in  $MPc$  (green/light gray lines here) do not change much. The  $d_{xz}$  and  $d_{yz}$  orbitals ( $|m| = 1$ ) of  $MnPc$ ,  $FePc$ , and  $CoPc$  shift slightly, while those of  $NiPc$ ,  $CuPc$ , and  $ZnPc$  remain almost unchanged. In the  $MnPc/Au(111)$ ,  $FePc/Au(111)$ , and  $CoPc/Au(111)$  systems, the black lines changed, which means that the  $d_{z^2}$  orbital plays an important role in the interaction between the  $MPc$  ( $M = Mn, Fe, \text{ or } Co$ ) molecules and the metal substrate. For the  $NiPc/Au(111)$ ,  $ZnPc/Au(111)$ , and  $CuPc/Au(111)$  systems, the  $d_{z^2}$  orbitals did not change that much. Now we can conclude that the  $MnPc$ ,  $FePc$ , and  $CoPc$  have stronger interactions with  $Au(111)$  than do  $NiPc$ ,  $CuPc$ , and  $ZnPc$ .

We performed an electron density difference analysis for two typical systems:  $MnPc/Au(111)$  as an example of relatively strong adsorption and  $ZnPc/Au(111)$  as an example of relatively weak adsorption. The integrated electron density difference in the  $x$ - $y$  plane is shown in Fig. 8. As described above, the adsorption of  $MnPc$  is stronger than that of  $ZnPc$ ,

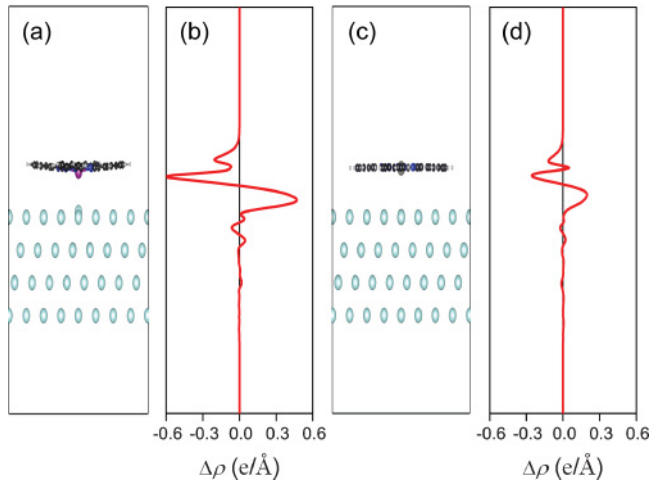


FIG. 8. (Color online) Integrated electron density difference for MnPc/Au(111) and ZnPc/Au(111) systems in a top-angle configuration. Side views of the adsorption configurations for the (a) MnPc/Au(111) system and (c) ZnPc/Au(111) system. Integrated electron density difference for the (b) MnPc/Au(111) system and (d) ZnPc/Au(111) system in the  $z$  direction. The charge transfer in the MnPc/Au(111) system is larger than in the ZnPc/Au(111) system. Negative  $\Delta\rho$  means electron loss, while positive  $\Delta\rho$  means electron accumulation.

and the geometric distortion for MnPc is larger than that of ZnPc, which can be seen in Figs. 8(a) and 8(c). It also shows clearly that the charge transfer in the MnPc/Au(111) system is

larger than that in the ZnPc/Au(111) system. Still, they follow the same pattern. This charge transfer induces a dipole moment perpendicular to the surface. The interactions among these dipole moments play an important role in the self-assembly behavior in this system.<sup>52</sup>

## VI. SUMMARY

The adsorption properties of  $3d$  transition-metal MPC molecules (MnPc, FePc, CoPc, NiPc, CuPc, and ZnPc) on a Au(111) substrate were investigated. We found that the small energy differences between different configurations allow the FePc molecules to diffuse easily on the substrate at certain temperatures, which is in good agreement with experimental observations. The electronic properties and the magnetic properties of the molecules on Au(111) were compared with those of the freestanding molecules. For all the molecules we studied, the electronic structures of the Pc skeleton do not change much as the molecules adsorb on Au(111). The magnetic properties of the central metal atoms are unchanged by adsorption for all the molecules except for CoPc.

## ACKNOWLEDGMENT

This work is supported by the National Science Foundation of China (Grant No. 10874219), National “973” Projects of China (Grant No. 2011CB808401), and Shanghai Supercomputer Center.

\*sxdu@iphy.ac.cn

†hjgao@iphy.ac.cn

<sup>1</sup>M. Eremtchenko, J. A. Schaefer, and F. S. Tautz, *Nature (London)* **425**, 602 (2003).

<sup>2</sup>S. X. Du, H. J. Gao, C. Seidel, L. Tsetseris, W. Ji, H. Kopf, L. F. Chi, H. Fuchs, S. J. Pennycook, and S. T. Pantelides, *Phys. Rev. Lett.* **97**, 156105 (2006).

<sup>3</sup>H. J. Gao and L. Gao, *Prog. Surf. Sci.* **85**, 28 (2010).

<sup>4</sup>J. V. Barth, G. Costantini, and K. Kern, *Nature (London)* **437**, 671 (2005).

<sup>5</sup>L. Gao *et al.*, *Phys. Rev. Lett.* **101**, 197209 (2008).

<sup>6</sup>X. Lu, K. W. Hipps, X. D. Wang, and U. Mazur, *J. Am. Chem. Soc.* **118**, 7197 (1996).

<sup>7</sup>K. W. Hipps, X. Lu, X. D. Wang, and U. Mazur, *J. Phys. Chem.* **100**, 11207 (1996).

<sup>8</sup>X. Lu and K. W. Hipps, *J. Phys. Chem. B* **101**, 5391 (1997).

<sup>9</sup>A. Zhao *et al.*, *Science* **309**, 1542 (2005).

<sup>10</sup>L. Gao *et al.*, *Phys. Rev. Lett.* **99**, 106402 (2007).

<sup>11</sup>Y.-S. Fu *et al.*, *Phys. Rev. Lett.* **99**, 256601 (2007).

<sup>12</sup>F. Petraki and S. Kennou, *Phys. Status Solidi C* **5**, 3708 (2008).

<sup>13</sup>M. Grobosch, V. Y. Aristov, O. V. Molodtsova, C. Schmidt, B. P. Doyle, S. Nannarone, and M. Knupfer, *J. Phys. Chem. C* **113**, 13219 (2009).

<sup>14</sup>A. F. Takács, F. Witt, S. Schmaus, T. Balashov, M. Bowen, E. Beaurepaire, and W. Wulfhekel, *Phys. Rev. B* **78**, 233404 (2008).

<sup>15</sup>G. V. Nazin, X. H. Qiu, and W. Ho, *Science* **302**, 77 (2003).

<sup>16</sup>N. Ogawa, G. Mikaelian, and W. Ho, *Phys. Rev. Lett.* **98**, 166103 (2007).

<sup>17</sup>G. Mikaelian, N. Ogawa, X. W. Tu, and W. Ho, *J. Chem. Phys.* **124**, 131101 (2006).

<sup>18</sup>N. Marom and L. Kronik, *Appl. Phys. A* **95**, 159 (2009).

<sup>19</sup>N. Marom and L. Kronik, *Appl. Phys. A* **95**, 165 (2009).

<sup>20</sup>N. Marom, O. Hod, G. E. Scuseria, and L. Kronik, *J. Chem. Phys.* **128**, 164107 (2008).

<sup>21</sup>N. Marom, A. Tkatchenko, M. Scheffler, and L. Kronik, *J. Chem. Theory Comput.* **6**, 81 (2010).

<sup>22</sup>V. Maslyuk, V. Aristov, O. Molodtsova, D. Vyalikh, V. Zhilin, Y. Ossipyan, T. Bredow, I. Mertig, and M. Knupfer, *Appl. Phys. A* **94**, 485 (2009).

<sup>23</sup>D. Stradi, C. Díaz, F. Martín, and M. Alcamí, *Theor. Chem. Acc.* **128**, 497 (2011).

<sup>24</sup>M. Marsman, J. Paier, A. Stroppa, and G. Kresse, *J. Phys. Condens. Matter* **20**, 064201 (2008).

<sup>25</sup>A. Stroppa, K. Termentzidis, J. Paier, G. Kresse, and J. Hafner, *Phys. Rev. B* **76**, 195440 (2007).

<sup>26</sup>J. D. Baran, J. A. Larsson, R. A. J. Woolley, Y. Cong, P. J. Moriarty, A. A. Cafolla, K. Schulte, and V. R. Dhanak, *Phys. Rev. B* **81**, 075413 (2010).

<sup>27</sup>Z. Hu, B. Li, A. Zhao, J. Yang, and J. G. Hou, *J. Phys. Chem. C* **112**, 13650 (2008).

- <sup>28</sup>N. Jiang, Y. Y. Zhang, Q. Liu, Z. H. Cheng, Z. T. Deng, S. X. Du, H.-J. Gao, M. J. Beck, and S. T. Pantelides, *Nano Lett.* **10**, 1184 (2010).
- <sup>29</sup>Q. Liu, Y. Y. Zhang, N. Jiang, H. G. Zhang, L. Gao, S. X. Du, and H.-J. Gao, *Phys. Rev. Lett.* **104**, 166101 (2010).
- <sup>30</sup>S. Grimme, *J. Comput. Chem.* **27**, 1787 (2006).
- <sup>31</sup>M. Dion, H. Rydberg, E. Schröder, D. C. Langreth, and B. I. Lundqvist, *Phys. Rev. Lett.* **92**, 246401 (2004).
- <sup>32</sup>A. Tkatchenko and M. Scheffler, *Phys. Rev. Lett.* **102**, 073005 (2009).
- <sup>33</sup>V. Barone, M. Casarin, D. Forrer, M. Pavone, M. Sambi, and A. Vittadini, *J. Comput. Chem.* **30**, 934 (2009).
- <sup>34</sup>J. Brede, N. Atodiresei, S. Kuck, P. Lazić, V. Caciuc, Y. Morikawa, G. Hoffmann, S. Blügel, and R. Wiesendanger, *Phys. Rev. Lett.* **105**, 047204 (2010).
- <sup>35</sup>R. Cuadrado, J. I. Cerdá, Y. Wang, G. Xin, R. Berndt, and H. Tang, *J. Chem. Phys.* **133**, 154701 (2010).
- <sup>36</sup>K. Tonigold and A. Groß, *J. Chem. Phys.* **132**, 224701 (2010).
- <sup>37</sup>G. Mercurio *et al.*, *Phys. Rev. Lett.* **104**, 036102 (2010).
- <sup>38</sup>E. R. McNellis, J. Meyer, and K. Reuter, *Phys. Rev. B* **80**, 205414 (2009).
- <sup>39</sup>K. Toyoda, Y. Nakano, I. Hamada, K. Lee, S. Yanagisawa, and Y. Morikawa, *J. Electron Spectrosc. Relat. Phenom.* **174**, 78 (2009).
- <sup>40</sup>K. Berland, T. L. Einstein, and P. Hyldgaard, *Phys. Rev. B* **80**, 155431 (2009).
- <sup>41</sup>Y. Zhang, W. Pan, and W. Yang, *J. Chem. Phys.* **107**, 7921 (1997).
- <sup>42</sup>G. Kresse and J. Hafner, *Phys. Rev. B* **47**, 558 (1993).
- <sup>43</sup>G. Kresse and J. Furthmüller, *Phys. Rev. B* **54**, 11169 (1996).
- <sup>44</sup>J. P. Perdew, J. A. Chevary, S. H. Vosko, K. A. Jackson, M. R. Pederson, D. J. Singh, and C. Fiolhais, *Phys. Rev. B* **46**, 6671 (1992).
- <sup>45</sup>P. E. Blöchl, *Phys. Rev. B* **50**, 17953 (1994).
- <sup>46</sup>G. Kresse and D. Joubert, *Phys. Rev. B* **59**, 1758 (1999).
- <sup>47</sup>M.-S. Liao and S. Scheiner, *J. Chem. Phys.* **114**, 9780 (2001).
- <sup>48</sup>K. A. Nguyen and R. Pachtter, *J. Chem. Phys.* **118**, 5802 (2003).
- <sup>49</sup>L. A. Zotti, G. Teobaldi, W. A. Hofer, W. Auwärter, A. Weber-Bargioni, and J. V. Barth, *Surf. Sci.* **601**, 2409 (2007).
- <sup>50</sup>J. V. Barth, H. Brune, G. Ertl, and R. J. Behm, *Phys. Rev. B* **42**, 9307 (1990).
- <sup>51</sup>W. Chen, V. Madhavan, T. Jamneala, and M. F. Crommie, *Phys. Rev. Lett.* **80**, 1469 (1998).
- <sup>52</sup>I. Fernandez-Torrente, S. Monturet, K. J. Franke, J. Fraxedas, N. Lorente, and J. I. Pascual, *Phys. Rev. Lett.* **99**, 176103 (2007).
- <sup>53</sup>Z. H. Cheng, L. Gao, Z. T. Deng, Q. Liu, N. Jiang, X. Lin, X. B. He, S. X. Du, and H.-J. Gao, *J. Phys. Chem. C* **111**, 2656 (2007).
- <sup>54</sup>L. Zhang *et al.*, *J. Phys. Chem. C* **115**, 10791 (2011).